Nonresonant Perturbation Measurements on Dispersion and Interaction Impedance Characteristics of Helical Slow-Wave Structures

S. J. Rao, S. Ghosh, P. K. Jain, and B. N. Basu

***Abstract*— A nonresonant perturbation (NRP) theory is developed from first principles for the measurement of dispersion and interaction impedance characteristics of a helical slow-wave structure (SWS). The phase of the reflected signal from a test helical structure varies when a perturber, also in the form of a helix, is moved along the axis of the test structure. The variation of phase with perturber position is interpreted to find the phase velocity of the structure under test. The interaction impedance of the structure is found by measuring the change in the axial phase-propagation constant of the structure as a dielectric rod is placed along the axis of the structure. For this purpose, first a "resonant" perturbation formula is derived for interaction impedance which, with proper interpretation, is then extended to get a "nonresonant" perturbation formula in terms of the above change in the axial phase-propagation constant. The formula shows an improvement over the first-order formula derived under "thin-rod approximations" in the form of a correction factor that takes into account the finite perturbation of the axial electric field inside the dielectric-rod perturber, the presence of a radial electric field, the nonuniformity of fields over the rod cross section, and the space-harmonic effects. However, the TE-field contributions are considered to be insignificant, thereby allowing one to ignore the presence of the azimuthal electric field. Measurements are carried out with the help of an automated setup using an HP 8510 vector network analyzer (VNA) and a PC to collect the phase informations for the various precisely controlled positions of the perturber using a stepper motor, which is also interfaced with the PC. The experimental and theoretical values of the phase velocity and the interaction impedance of a typical "cold" experimental helical structure for a wide-band TWT are found to be close within 0.5% and 5%, respectively, in an octave band of 8–16 GHz.**

***Index Terms*— Microwave measurement, nonresonant perturbation, slow-wave structure, traveling-wave tube.**

I. Introduction

THE UNIQUE combination of the gain and bandwidth offered by a traveling-wave tube (TWT) leaves it unrivaled as an amplifier in microwave communication systems, frequency agile wide-band electronic counter measure (ECM), and electronic counter-counter measure (ECCM) systems. The sub-assembly which demands utmost attention in the design of a broad-band TWT is the slow-wave structure (SWS). The extremely large bandwidth offered by a helical SWS is by far its most prominent claim to fame, and is unparalleled by any other known SWS's. The dispersion characteristics of a helix are required to be shaped by anisotropically and/or inhomogeneously loading the helix for a broad-band TWT [1]–[4]. However, care must be taken to see that the method of dispersion shaping does not cause a large reduction in the value of the interaction impedance of the structure, which in turn reduces the gain and efficiency of the device. Moreover, the method should not load the structure to such an extent that it causes a substantial reduction in the RF phase velocity, and hence, in the corresponding beam accelerating voltage and power. Furthermore, it should not reduce the π-point frequency—the potential backward-mode oscillation frequency—to a value below the upper edge of the desired amplification band [1]. Thus, the control of helix dispersion and impedance characteristics plays a significant role in the design of wide-band TWT's. Hence, this makes the experimental evaluation of a helical SWS—treated as a "cold" structure in the absence of an electron beam—with respect to these characteristics, using a simple, efficient, and speedy technique, crucially important from the TWT design and development considerations.

Both the resonant perturbation (RP) [5] and the non-RP (NRP) [6]–[10] techniques are in vogue for the experimental characterization of SWS's. However, for a helical SWS which cannot be perfectly "shorted" at its ends to make it resonate, the NRP technique is more suitable than the RP technique [5]. The NRP technique as applied to the experimental characterization of helical structures has been reported in the literature, for instance, by Legarra [6], Maharaj and Schumann [7], Onodera [8] and Wang *et al.* [9], [10].

As for the axial propagation constant, one may recall Steel's basic theory [11] that relates the change in the complex reflection coefficient at the measurement port of a nonresonant microwave cavity to the complex electric- and magnetic-field components at a given position on the cavity due to the insertion of a perturbing object at that position [11]. By using Steel's theory, one may thus obtain a simple NRP formula for the axial phase-propagation constant of a nonresonant helical structure in terms of the variation in the phase of the reflection coefficient as a perturber is moved along the structure axis (see Section II). For interaction impedance, Lagerstrom [12]

Manuscript received November 15, 1996; revised May 19, 1997.

The authors are with the Centre of Research in Microwave Tubes, Department of Electronics Engineering, Institute of Technology, Banaras Hindu University, Varanasi 221 005, India.

Publisher Item Identifier S 0018-9480(97)06062-6.

improved upon the original "first-order" formula based on "thin-rod approximations" not available in published literature, though presented in unpublished internal reports [13]–[14]. This prompts us in this paper to give a deduction of the NRP formula for interaction impedance from first principles removing such simplifying approximations for practical relevance. The approach used is to first deduce an RP formula following the approach of Horsley and Pearson [5], who gave it for a plane-ladder structure, and subsequently extend it to obtain the NRP formula for the present helical SWS (see Section II).

A computer-governed automated measurement setup, using a vector network analyzer (VNA) and a stepper motor for the precise control of the movement of a perturber is developed (see Section III) to collect the phase information as required in the formulas for the axial phase-propagation constant and the interaction impedance (see Section II) of a typical experimental helical structure in the 8–16-GHz range for a wide-band TWT. Finally, the experimental results are compared with those predicted by theoretical analyses previously developed by the authors [15]–[17] (see Section IV).

II. Theory of Measurement

The NRP formula for the axial phase-propagation constant β as required to study the dispersion characteristics of a helical structure is found by interpreting the variation of the phase of the reflected wave from the structure as a perturber is moved along the structure axis. As for the interaction impedance of the structure, first an RP formula is deduced, which by simple reasoning is then extended to obtain the desired NRP formula.

A. Dispersion Characteristics

Exploiting Steel's NRP theory [11], one may write the change $\Delta\Gamma\ (=|\Delta\Gamma|\exp(j\phi)$ in terms of its amplitude $|\Delta\Gamma|$ and phase $\phi)$ in the reflection coefficient at the measurement port of a nonresonant cavity as proportional to a generalized field quantity $p\ (=|p|\exp(-j\beta z)$ of amplitude $|p|$ and axial phase-propagation constant $\beta)$ at the perturber position z, in the following form [6]:

$$\begin{aligned}(\Delta\Gamma =)|\Delta\Gamma|\exp(j\phi)(=C[|p|\exp(-j\beta z)]^2)\\ = C|p|^2\exp(-j2\beta z)\end{aligned} \tag{1}$$

where C is a constant of proportionality. Differentiating (1) with respect to z and equating the imaginary part of its left-hand side (LHS) and right-hand side (RHS), one easily gets

$$\beta = -\frac{1}{2}\frac{d\phi}{dz} \tag{2}$$

from where one may find the phase velocity $v_p\ (=\omega/\beta)$ as

$$v_p = -\frac{2\omega}{(d\phi/dz)}. \tag{3}$$

From the variation of ϕ with the perturber position z along the axis of the structure, one may find $d\phi/dz$ and, hence, β from (2) or v_p from (3), as required for the experimental evaluation of the dispersion characteristics of the structure (see Sections III and IV).

B. Interaction Impedance Characteristics

Horsley and Pearson [5] gave a method of obtaining the RP formula for interaction impedance. They evaluated the perturbed electric field inside the perturber and the transverse-field effects by making electrostatic approximations. However, they ignored the variation of fields over the perturber cross section. Moreover, their theory referred to the measurement on a plane-ladder SWS which can be relatively easily shorted at its ends to form a resonant "cavity" suitable for RP measurements. Motivated by their work, we develop in this paper an NRP formula for interaction impedance from first principles with particular reference to a helical SWS. The approach is to first deduce the RP formula for interaction impedance [5] and then extend it to get the NRP formula. Unlike Horsley and Pearson [5], no electrostatic assumptions are made for the evaluation of the perturbed electric- and transverse-field effects. The NRP formula, as will be seen, gives an improvement over the first-order formula [12]–[14] in the form of a correction factor that accounts for: 1) the finite perturbation of the axial electric field inside the dielectric-rod perturber; 2) the presence of a radial electric field resulting from TM field (nonzero axial electric field) contributions; 3) the nonuniformity of fields over the perturber cross section; and 4) the space-harmonic effects due to the axial periodicity of the structure.

Let us recall the following well-known RP formula for a cavity of volume V in terms of $\Delta\omega$, the change in the angular frequency of resonance ω [18]:

$$\frac{\Delta\omega}{\omega} = \frac{\displaystyle\int_V(\hat{\boldsymbol{e}}\cdot\hat{\boldsymbol{D}}-\hat{\boldsymbol{E}}\cdot\hat{\boldsymbol{d}})\,dV - \int_V(\hat{\boldsymbol{h}}\cdot\hat{\boldsymbol{B}}-\hat{\boldsymbol{H}}\cdot\hat{\boldsymbol{b}})\,dV}{\displaystyle\int_V(\hat{\boldsymbol{E}}\cdot\hat{\boldsymbol{D}}-\hat{\boldsymbol{H}}\cdot\hat{\boldsymbol{B}})\,dV} \tag{4}$$

where the symbols $\boldsymbol{E}$, $\boldsymbol{H}$, $\boldsymbol{D}$, and $\boldsymbol{B}$ represent the unperturbed electric-field intensity, magnetic-field intensity, electric-flux density, and magnetic-flux density, respectively. The perturbations in these quantities are represented by the corresponding lower case symbols and the hats represent the amplitudes. If the relative permeability of the perturber is unity, one may write $\boldsymbol{h}\cdot\boldsymbol{B}=\boldsymbol{H}\cdot\boldsymbol{b}=\mu_0\boldsymbol{H}\cdot\boldsymbol{h}$ in the cavity volume that makes the second integral in the numerator of the RHS of (4) vanish, enabling one to write

$$\frac{\Delta\omega}{\omega} = \frac{\displaystyle\int_V(\hat{\boldsymbol{e}}\cdot\hat{\boldsymbol{D}}-\hat{\boldsymbol{E}}\cdot\hat{\boldsymbol{d}})\,dV}{\displaystyle\int_V(\hat{\boldsymbol{E}}\cdot\hat{\boldsymbol{D}}-\hat{\boldsymbol{H}}\cdot\hat{\boldsymbol{B}})\,dV}. \tag{5}$$

One may divide the volume V into the volumes V_p and $V-V_p$ where V_p represents the volume of the perturber, which in the present context refers to a thin dielectric perturbing rod at the axis of the helical structure. In view of this, one may choose to express (5) as

$$\frac{\Delta\omega}{\omega} = \frac{\displaystyle\int_{V-V_p}(\hat{\boldsymbol{e}}\cdot\hat{\boldsymbol{D}}-\hat{\boldsymbol{E}}\cdot\hat{\boldsymbol{d}})\,dV + \int_{V_p}(\hat{\boldsymbol{e}}\cdot\hat{\boldsymbol{D}}-\hat{\boldsymbol{E}}\cdot\hat{\boldsymbol{d}})\,dV}{\displaystyle\int_V(\hat{\boldsymbol{E}}\cdot\hat{\boldsymbol{D}}-\hat{\boldsymbol{H}}\cdot\hat{\boldsymbol{B}})\,dV}. \tag{6}$$

In order to approximately estimate the distortion of fields caused by a small perturber ($V_p \ll V$), one may use the usual approach of making the assumption that the perturbing object is placed in a region containing a replica of the original field pattern—frozen in the unperturbed condition [12]. Under this approximation, in the perturber-free volume $V - V_p$ one may take $\hat{\boldsymbol{e}} = \hat{\boldsymbol{d}} = 0$ that makes the integrand in the first integral of the numerator of the RHS of (6) vanish, giving

$$\frac{\Delta\omega}{\omega} = \frac{\int_{V_p} (\hat{\boldsymbol{e}} \cdot \hat{\boldsymbol{D}} - \hat{\boldsymbol{E}} \cdot \hat{\boldsymbol{d}})\, dV}{\int_V (\hat{\boldsymbol{E}} \cdot \hat{\boldsymbol{D}} - \hat{\boldsymbol{H}} \cdot \hat{\boldsymbol{B}})\, dV}. \tag{7}$$

Clearly, one may identify the denominator of the RHS of (7) as four times the total energy W stored in the unperturbed volume [5]. This enables one to write

$$\frac{\Delta\omega}{\omega} = \frac{\int_{V_p} (\hat{\boldsymbol{e}} \cdot \hat{\boldsymbol{D}} - \hat{\boldsymbol{E}} \cdot \hat{\boldsymbol{d}})\, dV}{4W}. \tag{8}$$

Representing the perturbed quantities by primed symbols, one may put $\hat{\boldsymbol{e}} = \hat{\boldsymbol{E}}' - \hat{\boldsymbol{E}}$ and $\hat{\boldsymbol{d}} = \hat{\boldsymbol{D}}' - \hat{\boldsymbol{D}}$, and write the integrand in (8) as

$$\hat{\boldsymbol{e}} \cdot \hat{\boldsymbol{D}} - \hat{\boldsymbol{E}} \cdot \hat{\boldsymbol{d}} = (\hat{\boldsymbol{E}}' - \hat{\boldsymbol{E}}) \cdot \hat{\boldsymbol{D}} - \hat{\boldsymbol{E}} \cdot (\hat{\boldsymbol{D}}' - \hat{\boldsymbol{D}}) = \hat{\boldsymbol{E}}' \cdot \hat{\boldsymbol{D}} - \hat{\boldsymbol{E}} \cdot \hat{\boldsymbol{D}}'$$

which, on putting $\hat{\boldsymbol{D}} = \varepsilon_0 \hat{\boldsymbol{E}}$ and $\hat{\boldsymbol{D}}' = \varepsilon_r \varepsilon_0 \hat{\boldsymbol{E}}'$, where ε_r is the relative permittivity of the perturber, becomes

$$\hat{\boldsymbol{e}} \cdot \hat{\boldsymbol{D}} - \hat{\boldsymbol{E}} \cdot \hat{\boldsymbol{d}} = -\varepsilon_0(\varepsilon_r - 1)\hat{\boldsymbol{E}}' \cdot \hat{\boldsymbol{E}}$$

which, when substituted in (8), gives

$$\frac{\Delta\omega}{\omega} = -\frac{\varepsilon_0(\varepsilon_r - 1)\int_{V_p} \hat{\boldsymbol{E}}' \cdot \hat{\boldsymbol{E}}\, dV}{4W}. \tag{9}$$

One may choose to express (9) in terms of instantaneous field intensities $\boldsymbol{E}'$ $(= \hat{\boldsymbol{E}}' \exp j(\omega t - \beta z))$ and $\boldsymbol{E}^*$ $(= \hat{\boldsymbol{E}} \exp -j(\omega t - \beta z))$, so that one may take $\hat{\boldsymbol{E}}' \cdot \hat{\boldsymbol{E}} = \boldsymbol{E}' \cdot \boldsymbol{E}^*$. This enables one to write (9) as

$$\frac{\Delta\omega}{\omega} = -\frac{\varepsilon_0(\varepsilon_r - 1)\int_{V_p} \boldsymbol{E}' \cdot \boldsymbol{E}^*\, dV}{4W} \tag{10}$$

where the asterisk represents the complex conjugate.

In the present context of a helical SWS, let the structure be perturbed by a thin dielectric rod positioned along its axis all along its length, the structure being considered as terminated in shorting planes at its ends to form a resonant cavity. Putting $W = 2UL = 2PL/v_g$ where U is the energy stored per unit length in each of the forward and backward traveling waves in such a cavity, $P\ (= Uv_g)$ the power in a propagating mode, and L the length of the dielectric-rod perturber, one may then express (10) as

$$\frac{\Delta\omega}{\omega} = -\frac{v_g\varepsilon_0(\varepsilon_r - 1)}{8PL}\int_{V_p} \boldsymbol{E}' \cdot \boldsymbol{E}^*\, dV. \tag{11}$$

Supposing now that in the helical structure considered, the TM mode dominates over the TE mode, one may consider $\boldsymbol{E}$ to be comprised of the axial E_z and the radial E_r components and no azimuthal component E_θ. In view of this, one may express (11) as

$$\frac{\Delta\omega}{\omega} = -\frac{v_g\varepsilon_0(\varepsilon_r - 1)}{8PL}\int_{V_p} (E_z' E_z^* + E_r' E_r^*)\, dV. \tag{12}$$

Though we have considered the space-harmonic effects later in this analysis, let us at this stage assume that only the zeroth-order nonazimuthally varying mode is perturbed by the placement of the dielectric rod. For such a mode, considering the axial electric-field intensity E_z to be comprised of the forward and backward components each of the same amplitude $\hat{E}_z$, which form a standing wave in the cavity, one may express (12), as explained in Appendix A, in the following form:

$$\frac{\Delta\omega}{\omega} = -\frac{v_g\pi\varepsilon_0(\varepsilon_r - 1)}{PL}\int_{r=0}^{r_p}\int_{z=0}^{L}\left[p_1 \cos^2\beta z\left(I_0\{\gamma r\} \cdot I_0\{\gamma' r\} + \frac{\beta^2}{\gamma\gamma'} I_1\{\gamma r\} I_1\{\gamma' r\}\right)\right]\hat{E}_z^2\{0\} r \cdot dr\, dz \tag{13}$$

where L is the length of the rod and r_p its radius. I_0 and I_1 are the modified Bessel functions of the first kind and of orders 0 and 1, respectively. γ and γ' are the unperturbed and the perturbed radial propagation constants given, respectively, by

$$\gamma = (\beta^2 - \omega^2\mu_0\varepsilon_0)^{1/2} = (\beta^2 - k^2)^{1/2}$$

and

$$\gamma' = (\beta^2 - \omega^2\mu_0\varepsilon_0\varepsilon_r)^{1/2} = \gamma\left(1 - \frac{k}{\gamma^2}(\varepsilon_r - 1)\right)^{1/2} = \gamma\left(1 - \frac{\varepsilon_r - 1}{(\beta/k)^2 - 1}\right)^{1/2} \tag{14}$$

where $k\ (= \omega(\mu_0\varepsilon_0)^{1/2})$ is the free-space propagation constant. p_1 is a factor relating the perturbed to the unperturbed field as

$$E_z'\{0\} = p_1 E_z\{0\} \tag{15}$$

where the expression for p_1 is given in Appendix B. The zero in the parenthesis with the electric-field quantity refers to the value of the quantity at the axis $r = 0$.

Taking the resonant length L as an integral multiple of half of the guide wavelength π/β, one gets

$$\int_{z=0}^{L(=\pi/\beta)} \cos^2\beta z\, dz = \frac{L}{2}$$

a result that can be used in (13) to get the RP expression for the interaction impedance $K\ (= \hat{E}_z^2\{0\}/(2\beta^2 P))$ as follows:

$$K = \frac{-2\Delta\omega}{\omega\beta^2 v_g \pi\varepsilon_0(\varepsilon_r - 1) r_p^2 p_1\left(p_2 + \dfrac{\beta^2}{\gamma\gamma'} p_3\right)} \tag{16}$$

where

$$p_2 = \frac{2}{r_p^2}\int_0^{r_p} r I_0\{\gamma r\} I_0\{\gamma' r\}\, dr \tag{17}$$

and

$$p_3 = \frac{2}{r_p^2}\int_0^{r_p} rI_1\{\gamma r\}I_1\{\gamma' r\}\,dr. \tag{18}$$

The evaluated expressions for p_2 and p_3 are given in Appendix B.

At this stage, one may extend the RP expression for the interaction impedance (16) to its NRP form using the following simple reasoning. A wave propagating through a nonresonant propagating structure will undergo a change in its axial phase-propagation constant by an amount $\Delta\beta$ due to the placement of the dielectric perturbing rod at the structure axis. This change is actually nullified in the RP condition by changing the excitation frequency so that the "cavity" now resonates at a new angular frequency $\omega+\Delta\omega$, thus introducing an additional change $(\partial\beta/\partial\omega)\Delta\omega$ in the axial phase-propagation constant. In other words, this means

$$0 = \Delta\beta + \frac{\partial\beta}{\partial\omega}\Delta\omega$$

and when remembering that the structure has a group velocity $v_g\ (=\partial\omega/\partial\beta)$, one gets $\Delta\omega = -v_g(\Delta\beta)$, which when substituted in (16) yields the following NRP expression for interaction impedance:

$$K = \left(\frac{1}{G_{p,nu,r}}\right)K_{\text{first-order}} \tag{19}$$

where

$$K_{\text{first-order}} = \frac{2\Delta\beta}{\omega\beta^2\pi\varepsilon_0(\varepsilon_r-1)r_p^2} \tag{20}$$

is the first-order expression for interaction impedance [12] that would be obtained had the effects of the field perturbation and nonuniformity, as well as those of the radial electric field, been ignored. Here

$$G_{p,nu,r} = p_1\left(p_2 + \frac{\beta^2}{\gamma\gamma'}p_3\right) \tag{21}$$

is a correction factor that takes into account the above effects.

It may be mentioned that the factor $G_{m,nu,r}$ does not include the space-harmonic effects which may now be considered as follows. In the presence of space harmonics other than the zeroth-order fundamental, one may define the fundamental interaction impedance K_0 as

$$K_0 = \frac{E_{z,0}^2\{0\}}{2\beta_0^2 P} \tag{22}$$

where $\hat{E}_{z,0}\{0\}$ is the amplitude of the zeroth-order fundamental-mode axial electric-field intensity at $r=0$, β_0 is the corresponding axial phase-propagation constant. P has to be taken here as the power propagating down the structure over all the space harmonics of interest. The effects of space harmonics on the interaction impedance formula may be estimated by referring to the results of tape-model analysis for the helix [15]–[17]. For instance, in the presence of space harmonics of orders ±1, one may write $\hat{E}_z\{0\}$

$$\hat{E}_z\{0\} = \hat{E}_{z,0}\{0\} + \hat{E}_{z,-1}\{0\} + \hat{E}_{z,1}\{0\}. \tag{23}$$

Consequently, it can be shown with the help of (23) and making use of the orthogonality property of space harmonics over the volume of the perturber, that the basic RP expression (13) then gets modified, shown in (24) at the bottom of the page (see Appendix C), where the subscript 0 with propagation constants referring to the zeroth-order fundamental space-harmonic mode. Here, the factor G_s is given by (see Appendix C)

$$G_s = 1 + S_{0,-1}^2 + S_{0,1}^2 \tag{25}$$

which may be expressed in the following generalized form:

$$G_s = 1 + \sum_{q=1}^{n} S_{0,-q}^2 + \sum_{q=1}^{n} S_{0,q}^2 \tag{26}$$

in the presence of harmonics $\pm1, \pm2, \cdots, \pm n$, where (see Appendix C)

$$S_{0,\pm q} = \frac{\hat{E}_{z,\pm q}\{0\}}{\hat{E}_{z,0}\{0\}} \tag{27}$$

is the relative $\pm q$th space-harmonic axial electric-field amplitude at the structure axis $(r=0)$ that can be found by the theoretical analysis of the structure in the tape model [15]–[17].

In view of the above modification of (13), in the form of (24), one may then follow the steps subsequent to (13), and hence, modify the NRP expression (19) to get the expression for the fundamental zeroth-order mode interaction impedance K_0 defined by (22) as follows:

$$K_0 = \left(\frac{1}{G_{p,nu,r}}\right)\left(\frac{1}{G_s}\right)K_{\text{first-order}} \tag{28}$$

where $G_{p,nu,r}$ is given by (21) in terms of p_1, p_2, and p_3 (the expressions of which are given in Appendix B) which may be interpreted for the zeroth-order mode, and G_s is given by (26) through (27) (see Appendix C), and $K_{\text{first-order}}$ being given by (20) interpreting β as β_0. It may be of interest to notice that (28) is identical with the first-order formula [12]–[14] except for the two factors $G_{p,nu,r}$, arising from the finite perturbation and nonuniformity of fields and the presence of a radial electric field in the perturber, and G_s, arising from the perturbation of space harmonics. Thus in (28), one gets an NRP formula for interaction impedance that gives an improvement over the first-order formula in the form of a correction factor $(1/G_{p,nu,r})(1/G_s)$. At this stage it may be mentioned that one could ignore the correction factors only

$$\frac{\Delta\omega}{\omega} = -\frac{v_g\pi\varepsilon_0(\varepsilon_r-1)G_s}{2PL}\int_{r=0}^{r_p}\int_{z=0}^{1}\left[p_1\cos^2\beta_0 z\left(I_0\{\gamma_0 r\}\cdot I_0\{\gamma_0' r\} + \frac{\beta_0^2}{\gamma_0\gamma_0'}I_1\{\gamma_0 r\}I_1\{\gamma_0' r\}\right)\right]\hat{E}_z^2\{0\}r\cdot dr\,dz \tag{24}$$

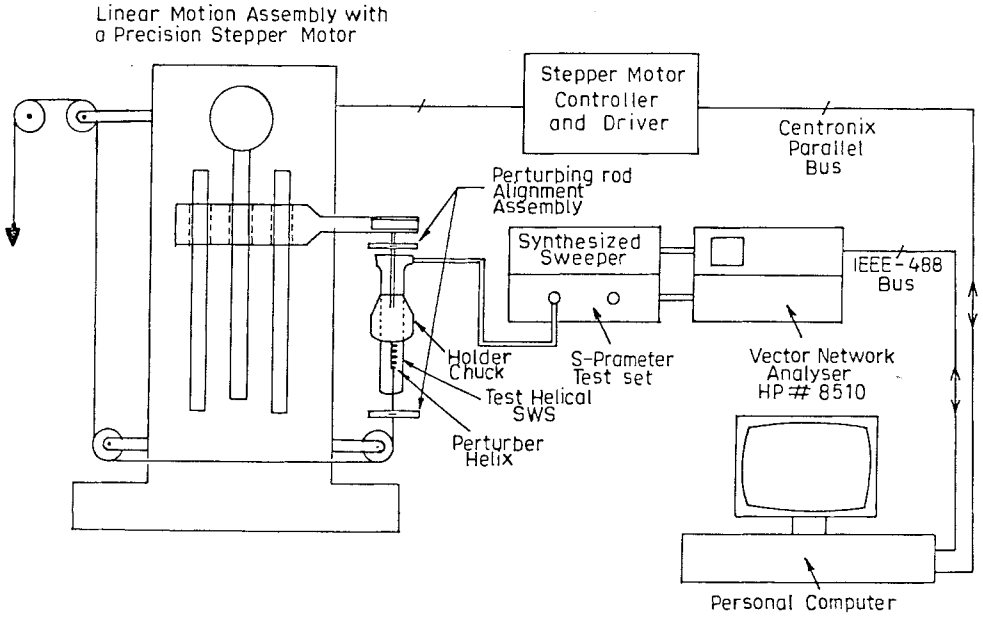

Fig. 1. Automated experiment setup for NRP measurement of the dispersion and interaction impedance characteristics of a helical SWS.

for thin low-permittivity small-perturbation dielectric rods. However, as could be seen from (20), this would demand that for $\Delta\beta$ to be discernible in the measurement, the value of K ought to be rather high. Therefore, this restriction on K in wider practical situations calls for the incorporation of these correction factors.

III. Experimental Setup

A setup is developed to automate the sequence of measurement on the dispersion and interaction impedance characteristics of a helical SWS with nominal user intervention (Fig. 1). An HP 8510 VNA is used to measure the phase of the reflected signal from the SWS at various frequencies. The phase changes when a perturber, in the form of a helix, is moved along the axis of the test helical SWS. The precise positioning of the perturber along the axis of the SWS is accomplished by a carriage assembly driven by a stepper motor. The carriage has a provision for holding the SWS and centering the perturber. The VNA is controlled by a PC via an IEEE-488 bus. The stepper motor is also interfaced on the centronix parallel port of the PC. A code is developed to control the measurement sequence in which the computer automatically collects the phase information of the reflected signal at the various positions of the perturber precisely controlled by the stepper motor. The PC collects and stores the data over a range of user-specified frequencies. Also, the computer is programmed to take another set of measurements on the helical SWS now loaded with a dielectric rod at its axis. The data stored in the PC are then processed making use of the NRP formulas developed in Section II to directly plot the dispersion and the interaction impedance characteristics of the helical SWS (see Figs. 2 and 3).

The design of the perturber used in the present measurement needs to be given special consideration taking care that it

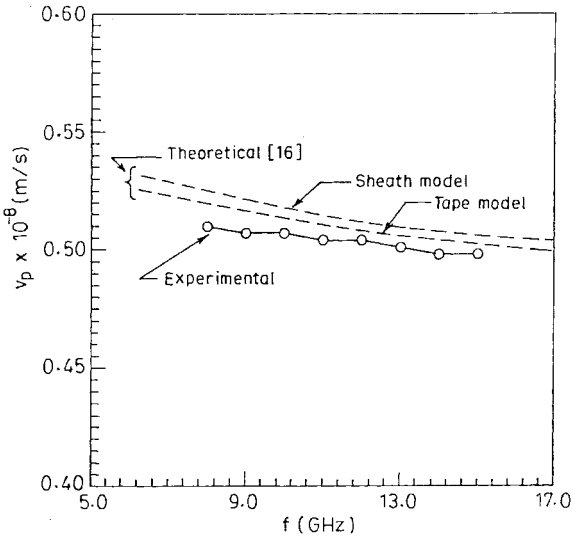

Fig. 2. A comparison between the theoretical and measured dispersion characteristics of a typical experimental helical SWS of a TWT.

behaves effectively throughout the frequency range of interest and is commensurate with the bandwidth of the test structure. As in Legarra [6], we have used here in the measurement a helical perturber. One important consideration in the design of a wide-band helical perturber is its optimum length for maximum power transfer, which should be constant with frequency [6], [8]. The deciding factors essentially are the separation between the test helix structure and the perturber helix, the relative permittivities of the materials present in the helical structure–perturber assembly, their dimensions including the ratio of the structure-to-perturber cotangents of helix pitch angle, the latter essentially being a negative quantity (≈ -0.98) corresponding to contra-wound coupled helixes [8], [19], [20]. Typically, a perturber helix of three turns of

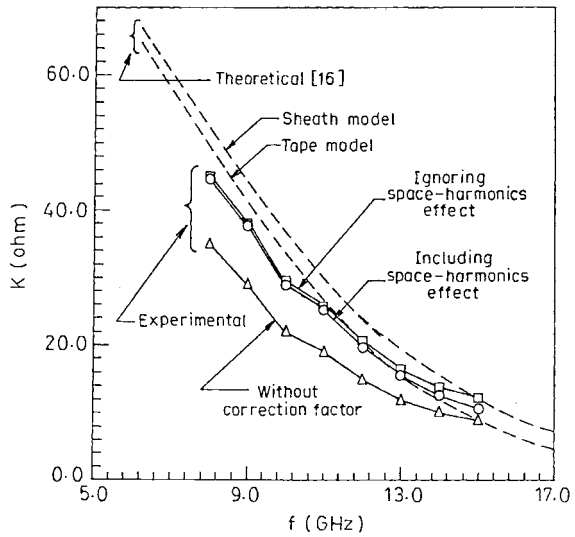

Fig. 3. Experimental interaction impedance characteristics with and without the correction factor compared with theory. Solid lines with circles and rectangles: inclusion and exclusion of the space harmonics, respectively, in the correction factor. Solid line with triangles: experimental values without a correction factor.

diameter equal to half the inner diameter of the test helix is found to give a broad-band perturbation. Furthermore, a good match between the helix terminal and the connecting cable of the VNA is essential for accurate measurements. The test structure used shows a VSWR between 1.2–1.8 over the 8–16-GHz band, which is improved further to give a VSWR of $\sim$ 1.05 using an additional triple-stub tuner, the residual mismatch being subtracted in the VNA during measurements by calibrating the VNA with the helix assembly taken as a matched load.

In order to measure the dispersion characteristics, the phase variation of the reflected signal ϕ as the perturber position z is changed, is used to obtain the value of $(d\phi/dz)$, which in turn gives the value of β and v_p using (2) and (3), respectively, at specified frequencies (Fig. 2). In order to evaluate the interaction impedance of the structure, the measurement is repeated after loading the helix by a thin dielectric rod at its axis. For this purpose, a glass rod of diameter 0.85 mm and relative permittivity 5.4 is used. Instead of sliding the perturber helix over the glass rod, the former is fixed on the latter, and the whole moved along the axis of the test helix taking care that both the ends of the glass rod remain outside the helix, to ensure that the end effects are avoided [12]. The new loaded axial propagation constant say, β', thus found gives $\Delta\beta\ (=\beta' - \beta)$, which in turn is used in (19), (20), and (28) to plot the experimental interaction impedance characteristics of the test helical SWS (Fig. 3). The repeatabilities in the measurement on dispersion and interaction impedance are found as $\sim$ 0.2% and $\sim$ 2%, respectively.

IV. Results and Discussion

The structure under test consists of a helix (mean radius = 1.09 mm, outer radius = 1.18 mm, tape width = 0.76 mm, pitch angle $=10.32^\circ$) supported by three identical anisotropic pyrolytic boron nitroide (APBN) (relative permittivity = 5.1), rectangular support bars (thickness = 0.59 mm) enclosed in a metal envelope (radius = 1.78 mm). The measurement is carried out using an automated computer-aided measurement setup (see Section III).

The experimental values of phase velocity closely agree (within $\sim$0.5%) with the theoretical values predicted by the author's previously published analysis [15]–[17], over a frequency range of 8–16 GHz (Fig. 2). As for interaction impedance, the first-order NRP formula is improved upon—in the first step, by taking into account the finite perturbation of the axial electric field inside the dielectric-rod perturber, the presence of a radial electric field, and the nonuniformity of fields over the rod cross section, and in the next step, also by taking into account the perturbation of the space harmonics of orders $\pm$ 1, $\pm$ 2, and $\pm$ 3, besides the zeroth-order fundamental, beyond which the results do not improve appreciably further (see Section II). The measured values of interaction impedance using the first-order formula and those using the same but improved by the two correction factors, as per the above steps, are compared with the theoretical values (Fig. 3). The experimental values of interaction impedance as found using the first-order formula appreciably differ (maximum $\sim$ 30%) from the theoretical values found by the author's analysis reported elsewhere [16], [17], more so at lower frequencies. However, the agreement becomes much closer (within $\sim$ 2%) when both the correction factors are taken into account (Fig. 3). It may be further noted that the inclusion of the correction factor due to the space harmonics lowers the value of the interaction impedance, though not to an appreciable extent (Fig. 3), as also has been observed by Wang *et al.* [9]. It is, however, felt that this factor would cause an appreciable effect for large helix pitch angles, a heavy loading of the helix, say, by a high permittivity or a thick dielectric support, and at high operating frequencies.

V. Conclusions

This paper reports an automatic measurement setup for the characterization of nonresonant structures. The background NRP theory of measurement for this purpose is developed from first principles. The formula deduced for interaction impedance takes into account the perturbation of the axial field inside the dielectric-rod perturber, the presence of a radial electric field, the nonuniformity of fields over the rod cross section, and also the perturbation of the space harmonics. The experimental results are validated against theory. It may be mentioned that there is a scope further to improve the results on interaction impedance by eliminating the effect of TE-field contributions in the measurement [12]. This could be done by repeating the experiment by a metal rod in lieu of a dielectric-rod perturber, and subsequently combining the results of the dielectric- and metal-rod experiments [12]. It is hoped that the NRP theory and the measurement technique based thereon and developed in this paper, should be useful in the design and characterization of helical structures—for instance, those used by tube developers in wide-band TWT's.

APPENDIX A
INTEGRAL FORM OF RESONANT PERTURBATION EXPRESSION

For the zeroth-order nonazimuthally varying mode, one may write for fields inside the perturber [12] as follows:

$$E_z = E_z\{0\} I_0\{\gamma r\} \exp j(\omega t - \beta z)$$
$$E_z' = E_z'\{0\} I_0\{\gamma' r\} \exp j(\omega t - \beta z)$$
$$E_r = \frac{j\beta}{\gamma} E_z\{0\} I_1\{\gamma r\} \exp j(\omega t - \beta z) = \frac{j\beta}{\gamma} \frac{I_1\{\gamma r\}}{I_0\{\gamma r\}} E_z$$

and

$$E_r' = \frac{j\beta}{\gamma'} E_z'\{0\} I_1\{\gamma' r\} \exp\, j(\omega t - \beta z) = \frac{j\beta}{\gamma'} \frac{I_1\{\gamma' r\}}{I_0\{\gamma' r\}} E_z' \tag{A.1}$$

where I_0 and I_1 are the modified Bessel functions of the first kind and of orders 0 and 1, respectively. The prime refers to the perturbed quantities.

Substituting E_z' and E_r' from (A.1), and E_z^* and E_r^*, also obtainable from (A.1), into (12) one may then write

$$\frac{\Delta\omega}{\omega} = -\frac{v_g \varepsilon_0 (\varepsilon_r - 1)}{8PL} \int_{V_p} E_z' E_z^* \cdot \left(1 + \frac{\beta^2}{\gamma\gamma'} \frac{I_1\{\gamma r\} I_1\{\gamma' r\}}{I_0\{\gamma r\} I_0\{\gamma' r\}}\right) dV. \tag{A.2}$$

Now, taking E_z to be composed of the forward and backward waves of the same amplitude $\hat{E}_z$ which form a standing wave in the cavity, one may represent E_z as

$$E_z = \hat{E}_z(\exp j(\omega t - \beta z) + \exp j(\omega t + \beta z)) = 2\hat{E}_z \cos \beta z \exp(j\omega t) \tag{A.3}$$

from where one may write

$$E_z' = 2\hat{E}_z' \cos \beta z \exp(j\omega t) \tag{A.4}$$

and

$$E_z^* = 2\hat{E}_z \cos \beta z \exp(-j\omega t). \tag{A.5}$$

Substituting (A.4) and (A.5) into (A.2), one gets

$$\frac{\Delta\omega}{\omega} = -\frac{v_g \varepsilon_0 (\varepsilon_r - 1)}{2PL} \int_{V_p} \hat{E}_z \hat{E}_z' \cos^2 \beta z \cdot \left(1 + \frac{\beta^2}{\gamma\gamma'} \frac{I_1\{\gamma r\} I_1\{\gamma' r\}}{I_0\{\gamma r\} I_0\{\gamma' r\}}\right) dV. \tag{A.6}$$

Assuming that the perturbing object is placed in a region of the original field "frozen" in the unperturbed condition [12], as discussed following (6), one may relate the perturbed quantity $\hat{E}_z'\{0\}$, to the corresponding unperturbed quantity $\hat{E}_z\{0\}$, both taken at the structure axis $r = 0$, by a factor p_1 (15). The expression for p_1 is given in Appendix B. With the help of (15) and (A.1), one may then express (A.6) as

$$\frac{\Delta\omega}{\omega} = -\frac{v_g \varepsilon_0 (\varepsilon_r - 1)}{2PL} \int_{V_p} \left[p_1 \cos^2 \beta z \left(I_0\{\gamma r\} \cdot I_0\{\gamma' r\} + \frac{\beta^2}{\gamma\gamma'} I_1\{\gamma r\} I_1\{\gamma' r\}\right)\right] \hat{E}_z^2\{0\}\, dV. \tag{A.7}$$

Now, putting the element of volume $dV = 2\pi r\, dr\, dz$ in (A.7) and taking the integration extended over the volume of the perturbing rod between $r = 0$ and $r = r_p$ (rod radius) and $z = 0$ and $z = L$ (rod length), one obtains the RP expression shown in (13).

APPENDIX B
EXPRESSIONS FOR p_1, p_2, AND p_3

Expression for $p_1 = E_z'\{0\}/E_z\{0\}$ may be found from the boundary-value problem of the helix internally loaded by a coaxial dielectric-rod perturber. For a nonazimuthally varying mode, the relevant field expressions are [12]

$$E_{z1} = A_1 I_0\{\gamma' r\} \tag{B.1}$$
$$E_{z2} = A_2 I_0\{\gamma r\} + B_2 K_0\{\gamma r\} \tag{B.2}$$
$$H_{\theta 1} = \frac{j\omega\varepsilon_0\varepsilon_r}{\gamma'} A_1 I_1\{\gamma' r\} \tag{B.3}$$
$$H_{\theta 2} = \frac{j\omega\varepsilon_0}{\gamma'} (A_2 I_1\{\gamma r\} - B_2 K_1\{\gamma r\}), \tag{B.4}$$

where the subscript 1 refers to the region inside the dielectric perturbing rod and subscript 2 refers to the region between the rod and the helix treated as a "helical sheath" in the well-known sheath-helix model. A and B are the field constants.

Now, if it is assumed that the dielectric-rod perturber is "frozen" in the unperturbed condition, one may find $E_z\{0\}$ the unperturbed axial electric-field intensity at $r = 0$, as the field intensity E_{z2} "stretched" up to $r = 0$. Thus, with the help of (B.2), in which B_2 now has to be interpreted as zero so that the field does not blow up at $r = 0$ where the function $K_0\{\gamma r\} \to \infty$, one gets

$$E_z\{0\} = A_2. \tag{B.5}$$

The perturbed field intensity $E_z'\{0\}$ is obtained as the field intensity E_{z1} taken at $r = 0$ and is given with the help of (B.1) as

$$E_z'\{0\} = A_1. \tag{B.6}$$

p_1 is then identified with the help of (B.5) and (B.6) as

$$p_1 = \frac{E_z'\{0\}}{E_z\{0\}} = \frac{A_1}{A_2}. \tag{B.7}$$

In order to find the ratio A_1/A_2 one may take help from the following two boundary conditions at $r = r_p$, the interface between the dielectric rod and the free-space region outside the dielectric

$$(E_{z1})_{r=b} = (E_{z2})_{r=b} \tag{B.8}$$

and

$$(H_{\theta 1})_{r=b} = (H_{\theta 2})_{r=b}. \tag{B.9}$$

Substituting (B.1)–(B.4) into (B.8) and (B.9), one gets

$$A_1 I_0\{\gamma' r_p\} = A_2 I_0\{\gamma r_p\} + B_2 K_0\{\gamma r_p\}$$

and

$$\frac{j\omega_0\varepsilon_0\varepsilon_r}{\gamma'} A_1 I_1\{\gamma' r_p\} = \frac{j\omega\varepsilon_0}{\gamma} (A_2 I_1\{\gamma r_p\} - B_2 K_1\{\gamma r_p\})$$

respectively, from which one may eliminate B_2 to get the ratio A_1/A_2 which is equal to p_1, as can be seen from (B.7). Thus we have

$$p_1\left(=\frac{A_1}{A_2}\right) = \frac{1}{\gamma r_p\left(K_1\{\gamma r_p\}I_0\{\gamma' r_p\}+\frac{\gamma}{\gamma'}\varepsilon_r K_0\{\gamma r_p\}I_1\{\gamma' r_p\}\right)}.$$

The expression for p_2 and p_3 given by (17) and (18), respectively, after evaluation of the definite integrals occurring therein, are [12]

$$p_2 = I_0\{\gamma r_p\}I_0\{\gamma' r\}\left[\frac{2I_1\{\gamma' r_p\}}{\gamma' r_p I_0\{\gamma' r_p\}}+\frac{1}{\varepsilon_r-1}\cdot\left(\frac{\gamma}{k}\right)^2\left(\frac{2I_1\{\gamma' r_p\}}{\gamma' r_p I_0\{\gamma' r_p\}}-\frac{2I_1\{\gamma r_p\}}{\gamma r_p I_0\{\gamma r_p\}}\right)\right]$$

and

$$p_3 = \frac{I_0\{\gamma r_p\}I_0\{\gamma' r_p\}}{\{\varepsilon_r-1\}}\left[\frac{2I_1\{\gamma' r_p\}}{\gamma' r_p I_0\{\gamma' r_p\}}-\frac{2I_1\{\gamma r_p\}}{\gamma r_p I_0\{\gamma r_p\}}\right].$$

Appenidx C
Expression for G_s

Considerable simplification is achieved if it is assumed that the quantity under the third bracket in the integrand of (24) would not change from harmonic to harmonic, though now $\hat{E}_z\{0\}$ is comprised of harmonics ± 1, say, in addition to the zeroth-order fundamental as given by (23). Thus, in view of (23), one may write the integral

$$\begin{aligned}\int_{V_p}\hat{E}_z^2\{0\}\,dV &= \int_{V_p}(\hat{E}_{z,0}\{0\}+\hat{E}_{z,-1}\{0\}+\hat{E}_{z,1}\{0\})^2\,dV\\ &= \int_{V_p}(\hat{E}_{z,0}^2\{0\}+\hat{E}_{z,-1}^2\{0\}+\hat{E}_{z,1}^2\{0\})\,dv\\ &\quad+2\int_{V_p}(\hat{E}_{z,0}\{0\}\hat{E}_{z,-1}\{0\}+\hat{E}_{z,0}\{0\}\hat{E}_{z,1}\{0\}\\ &\quad+\hat{E}_{z,-1}\{0\}\hat{E}_{z,1}\{0\})\,dV. \qquad \text{(C.1)}\end{aligned}$$

The second integral of (C.1) vanishes in view of the orthogonality relation of space harmonics, giving

$$\begin{aligned}\int_{V_p}\hat{E}_z^2\{0\}\,dV &= \int_{V_p}(\hat{E}_{z,0}^2\{0\}+\hat{E}_{z,-1}^2\{0\}+\hat{E}_{z,1}^2\{0\})\,dV\\ &= \int_{V_p}G_s\hat{E}_{z,0}^2\{0\}\,dV \qquad \text{(C.2)}\end{aligned}$$

where G_s is given by (25), for the harmonics ± 1 considered in addition to the zeroth-order fundamental, and it is given by (26) if the harmonics $\pm 1, \pm 2, \cdots, \pm n$ other than the zeroth-order fundamental are considered. The ratio $S_{0,\pm q}$ given by (27) as required to find G_s may be found from the tape-helix analysis [16], [17]. The latter can be found assuming a suitable tape-current distribution in the model. For instance, it will be reasonable to assume that the amplitude of the tape-surface current density taken parallel to the winding direction is constant over the tape width and that its phase varies in the direction of winding of the tape according to the phase factor $\exp(-j\beta_0 z)$, where z corresponds to a point moving along the center line of the tape. Then directly from the tape-helix analysis [15]–[17], the following relation is obtained for a helix surrounded by a dielectric tube of an effective relative permittivity ε_r' into which the discrete dielectric support rods for the helix could be azimuthally smoothed out, the whole enclosed in a metal envelope:

$$\begin{aligned}S_{0,\pm q} &= \frac{\gamma_{\pm q}^2 K_{\pm q}\{\gamma_{\pm q}a\}\left(\sin\psi-\frac{\pm q\beta_{\pm q}\cos\psi}{\gamma_{\pm q}^2 a}\right)}{\gamma_0^2 K_0\{\gamma_0 a\}\sin\psi}\\ &\quad\cdot\frac{F_{\pm q}}{F_0}\frac{\sin(\beta_{\pm q}\delta/2)}{\sin(\beta_0\delta/2)}\frac{\beta_0}{\beta_{\pm q}} \qquad \text{(C.3)}\end{aligned}$$

where

$$\begin{aligned}F_{\pm q} &= \left[1-\frac{I_{\pm q}\{\gamma_{\pm q}a\}K_{\pm q}\{\gamma_{\pm q}c\}}{K_{\pm q}\{\gamma_{\pm q}a\}I_{\pm q}\{\gamma_{\pm q}c\}}\right]\\ &\quad\cdot\left[1-(\varepsilon_r'-1)\gamma_{\pm q}aI_{\pm q}\{\gamma_{\pm q}a\}K_{\pm q}'\{\gamma_{\pm q}a\}\right.\\ &\quad\left.\cdot\left(1-\frac{I_{\pm q}'\{\gamma_{\pm q}a\}K_{\pm q}\{\gamma_{\pm q}c\}}{K_{\pm q}'\{\gamma_{\pm q}a\}I_{\pm q}\{\gamma_{\pm q}c\}}\right)\right]^{-1}\\ F_0 &= \left[1-\frac{I_0\{\gamma_0 a\}K_0\{\gamma_0 c\}}{K_0\{\gamma_0 a\}I_0\{\gamma_0 c\}}\right]\\ &\quad\cdot\left[1-(\varepsilon_r'-1)\gamma_0 aI_0\{\gamma_0 a\}K_0'\{\gamma_0 a\}\right.\\ &\quad\left.\cdot\left(1-\frac{I_0'\{\gamma_0 a\}K_0\{\gamma_0 c\}}{K_0'\{\gamma_0 a\}I_0\{\gamma_0 c\}}\right)\right]^{-1}\\ \gamma_{\pm q} &= (\beta_{\pm q}^2-k^2)^{1/2},\quad \gamma_0=(\beta_0^2-k^2)^{1/2}\end{aligned}$$

and $\beta_{\pm q}=\beta_0\pm q\cot\psi/a$, ψ and a being the helix pitch angle and mean radius, respectively, and c the metal envelope radius. $I_{\pm q}$ and $K_{\pm q}$ are the modified Bessel functions of the first and second kinds of order $\pm q$, respectively, and the primes denote their derivatives with respect to arguments.

$S_{0,\pm q}$, and hence G_s, being independent of volume of the perturber may be taken outside the integral in the RHS of (C.2) enabling one to write

$$\int_{V_p}\hat{E}_z^2\{0\}\,dV = G_s\int\hat{E}_{z,0}^2\{0\}\,dV. \qquad \text{(C.4)}$$

Therefore, in view of (C.4), the RP expression (13) gets modified as (24) [as discussed, following (23)].

References

[1] J. L. Putz and M. J. Cascone, "Effective use of dispersion shaping as a design parameter in broad-band helix TWT circuits," in *IEEE Int. Electron. Devices Meeting Tech. Dig.*, Washington, DC, Dec. 1979, pp. 422–424.

[2] P. Galuppy and M. D. Salvatore, "Evaluation of three techniques of controlling phase velocity dispersion in helix TWT," in *Proc. Int. Conf. Microwave Tubes in Systems: Problems and Prospects*, London, U.K., Oct. 1984, pp. 59–62.

[3] P. Galuppy and C. Lamesa, "A new technique for ultra-broad-band high power TWT's," *Military Microwave Conf. Proc.*, vol. MM-80, pp. 501–505, 1980.

[4] E. F. Belohoubek, "Helix support structure for ultra-wide-band travelling-wave tubes," *RCA Rev.*, vol. 26, pp. 106–117, 1965.

[5] A. W. Horsley and A. Pearson, "Measurement of dispersion and interaction impedance characteristics of slow-wave structures by resonance

methods," *IEEE Trans. Electron Devices*, vol. ED-13, pp. 962–969, 1962.
[6] J. R. Legarra, "Measurement of microwave characteristics of helix travelling wave circuits," in *IEEE Int. Electron Devices Meeting Tech. Dig.*, Washington, DC, Dec. 1979, pp. 408–411.
[7] B. T. Maharaj and E. W. Schumann, "Automated measurement methods to characterize travelling-wave tube slow-wave structure," *Elektron*, (South Africa), vol. 6, pp. 8–10, 1989.
[8] T. Onodera and K. C. Tucker, Optimum dimensions of perturbers for measuring microwave characteristics of helix traveling wave circuits," in *Proc. 4th Int. Symp. Recent Trends Microwave Technol.*, New Delhi, India, Dec. 1993, pp. 422–425.
[9] P. Wang, R. G. Carter, and B. N. Basu, "An improved technique for measuring the Pierce impedance of helix slow-wave structures," in *Proc. 24th European Microwave Conf.*, vol. 2, Cannes, France, Sept. 1994, pp. 998–1003.
[10] P. Wang, R. G. Carter, B. N. Basu, and A. K. Sinha, "A simple technique for measuring the Pierce impedance of the helical slow-wave structures for TWT's," presented at the *ITG Conf.*, Germany, 1995.
[11] C. W. Steele, "A nonresonant perturbation theory," *IEEE Trans. Microwave Theory Tech.*, vol. MTT-14, pp. 70-74, 1966.
[12] R. P. Lagerstrom, "Interaction impedance measurements by perturbation of travelling waves," Electron. Res. Laboratory, Stanford Univ., Stanford, CA, Rep. 7, 1957.
[13] E. T. Jaynes, "Advanced microwave theory I," unpublished.
[14] J. R. Klander, "A method for measuring impedance in traveling-wave tubes," Bell Telephone Laboratories Memorandum, New York, NY, MM-54-2144-20, 1954.
[15] A. K. Sinha, R. Verma, R. K. Gupta, L. Kumar, S. N. Joshi, P. K. Jain, and B. N. Basu, "Simplified tape model of arbitrary-loaded helical slow-wave structures of a traveling-wave tube," *Proc. Inst. Elect. Eng.*, vol. 139, pt. H, pp. 347–350, 1992.
[16] S. Ghosh, P. K. Jain, and B. N. Basu, "Rigorous tape analysis of inhomogeneously loaded helical slow-wave structure," *IEEE Trans. Electron Devices*., to be published.
[17] S. Ghosh, "Analytical studies on inhomogeneously loaded helical structures for broad-band TWT's," Ph.D. dissertation, Dept. Electron. Eng., Banaras Hindu Univ., Varanasi, India, 1996.
[18] R. A. Waldran, *Theory of Guided Electromagnetic Waves*. New York: Van Nostrand, 1970.
[19] S. Cook, R. Kompfner, and C. F. Quate, "Coupled helices," *Bell Syst. Tech. J.*, vol. 35, pp. 127–178, 1956.
[20] V. N. Singh, B. N. Basu, B. B. Pal, and N. C. Vaidya, "Equivalent circuit analysis of a system of coupled helix transmission line in a complex environment," *J. Appl. Phys.*, vol. 54, pp. 4141–4146, 1983.

S. J. Rao was born in Kakinada, India, on October 23, 1973. He received the B.Tech degree in electronics engineering from the Institute of Technology, Banaras Hindu University (BHU), Varanasi, India, in 1996.

His research interest includes high-power fast-wave electron beam devices, particularly gyro-TWT amplifiers and CAD/CAM. He has authored or co-authored numerous research papers published in journals and presented at various national conferences.

S. Ghosh was born in Midnapur, India, in 1966. He received the B.Sc. degree from Banaras Hindu University (BHU), Varanasi, India, in 1991, and is currently working toward the Ph.D. degree.

His research interest include analysis and modeling of TWT's and its subassemblies.

P. K. Jain received the B.Tech. degree (in electronics engineering) and the M.Tech. and Ph.D. degrees (in microwave engineering), all from Banaras Hindu University (BHU), Varanasi, India, in 1979, 1981, and 1988, respectively.

In 1981, he joined the Centre of Research in Microwave Tubes (CRMT), Department of Electronics Engineering, Institute of Technology, (BHU), as a Lecturer, and is currently working there as a Reader. His current areas of research and publication include CAD/CAM and modeling of microwave tubes and their subassemblies, high-power radiation from cyclotron resonance masers, including gyro-TWT's.

Dr. Jain is a fellow of the Institution of Electronics and Telecommunication Engineers (India).

B. N. Basu received the M.Tech. and Ph.D. degrees from the Institute of Radiophysics and Electronics, Calcutta University, Calcutta, India, in 1966 and 1976, respectively.

He had been associated with the Institute of Radiophysics and Electronics, Calcutta, the Defence Electronics Research Laboratory, Hyderabad, the Indian Institute of Technology, Kharagpur, the Regional Institute of Technology, Jamshedpur, and the Central Electronics Engineering Research Institute (CEERI), Pilani. He is currently working as a Professor and Coordinator at the Centre of Research in Microwave Tubes (CRMT), Electronics Engineering Department, Banaras Hindu University (BHU), Varanasi, India. He is also professionally associated with CEERI, Pilani, as a Distinguished Visiting Scientist/Short-Term Consultant of Council of Scientific and Industrial Research (CSIR), India, and has been seconded by CSIR and the British Council to work at the University of Lancaster, Lancaster, U.K., under an academic-link program. He has authored a book entitled *Electromagnetic Theory and Applications in Beam-Wave Electronics* (World Scientific, Singapore), and has appeared in the 14th edition of *Marquis Who's Who in the World*. His areas of current interest and publications include helix-TWT modeling, broad-banding of TWT's, synthesis of electron guns, and gyro-TWT amplifiers.